Inorganic Materials, Vol. 39, No. 11, 2003, pp. 1147–1153. Translated from Neorganicheskie Materialy, Vol. 39, No. 11, 2003, pp. 1329–1336.
Original Russian Text Copyright © 2003 by Matzui, Vovchenko, Kapitanchuk, Zakharenko, Babich.

C–Co Nanocomposite Materials

L. Yu. Matzui, L. L. Vovchenko, L. M. Kapitanchuk,
N. I. Zakharenko, and N. G. Babich
Shevchenko National University, Vladimirskaya ul. 64, Kiev, 03033 Ukraine
e-mail: vovch@mail.univ.kiev.ua

Received December 27, 2002; in final form, April 23, 2003

Abstract—The formation of cobalt particles on the surface of graphite supports via salt thermolysis is studied by x-ray diffraction, electron microscopy, Auger electron spectroscopy, and secondary ion mass spectrometry. The results demonstrate that each step in the fabrication of graphite–cobalt composites causes changes in the particle size, phase composition, and morphology of the deposit. The process involves the formation of a thin, fine-grained salt film on the surface of thermally expanded graphite particles as a result of impregnation; thermal decomposition of the salt, leading to the formation of crystalline cobalt oxide particles 50 to 100 nm in size, uniformly distributed over the surface of thermally expanded graphite; and the formation of Co particles on the graphite surface. The Co particles are 60–70 to 150 nm in size and form aggregates up to 400 nm in size.

INTRODUCTION

Materials containing nanocrystalline components or consisting of nanoparticles have recently been intensely studied because they exhibit unusual physical properties. The relatively large fraction of surface atoms in particles 1 to 30 nm in size results in specific properties of such particles and related nanocrystalline systems. For example, in a particle 5 nm in diameter, 15% of the atoms are situated in the top surface layer [1–3]. Surface atoms have an increased energy and differ markedly in energy state from interior atoms. As a consequence, the properties of nanoparticles and nanocrystalline materials differ significantly from those of bulk materials. The surface atoms of nanoparticles enhance their capacity for adsorption, atomic and ion exchange, and contact interactions between structural elements and determine their structural transitions and melting point. Nanocrystalline materials with a large interface area possess an excess energy compared to homogeneous materials and are, therefore, high-energy, pyrophoric systems [4].

The morphology, dispersity, atomic structure, and properties of nanoparticles depend significantly on their composition, the preparation procedure, and the environment. Nanocrystalline materials are often produced by attaching metallic nanoparticles to the surface of supports. The use of various types of supports for metallic or metal-oxide nanoparticles extends the range of suitable particle sizes and influences the particle distribution over the support surface, thereby extending the range of physical properties of the resulting materials. A wide variety of approaches are used to fabricate nanocomposites. One of the widely used chemical techniques is the thermolysis of metal salts [2, 3]. In this technique, supports must meet a number of requirements:

high specific surface area and highly porous structure, which facilitate the impregnation of the support with metal-salt solutions [4];

the presence of oxygen-containing groups, which act as active centers for the nucleation of metal particles (usually, these are phenol, carboxy, lactone, and ketone groups on graphite [5, 6]; in addition, a certain relationship between oxidizing and reducing groups is necessary [4]);

nonreactivity with metals and metal compounds (to ensure stability of the composite).

The purpose of this work was to investigate the formation of the metallic component on the surface of graphite supports in the fabrication of graphite–cobalt composites via salt thermolysis and to assess the effects of particular process steps on the distribution, particle size, and phase composition of the material.

EXPERIMENTAL

As the support material, we used thermally expanded graphite (TEG), which was prepared by thermochemical treatment of natural graphite [7] and met all of the above requirements for supports.

To prepare TEG–metal materials, we used deposition of metal salts from aqueous salt solutions, followed by thermal decomposition of the salt to the metal or a metal oxide [2, 3]. In the TEG–Co system, cobalt acetate was used as the Co precursor.

Cobalt was deposited onto graphite supports in several steps.

The first step was surface preparation. TEG is a highly porous material (apparent density of 3 kg/m^3), with a large, reactive surface. To enhance the activity of

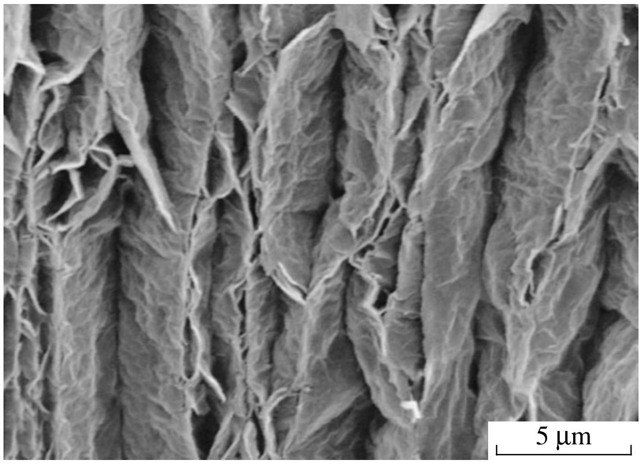

Fig. 1. Fragment of a TEG particle after sulfuric acid oxidation and thermal shock at 800°C.

the TEG surface, the material was impregnated with sulfuric acid and then dried at 100–120°C.

TEG oxidation leads to the formation of oxygen-containing surface groups, which act as exchange centers for fixing cations on the surface of the TEG–metal (or TEG–metal oxide) composite and raise the density of surface defects. In addition, oxidation produces surface asperities, which also act as active centers for fixing metal ions [5, 6]. Moreover, sulfuric acid may intercalate into graphite, leading to its expansion during subsequent heat treatment.

The second step was the impregnation of the oxidized graphite material with an aqueous solution of cobalt acetate under certain conditions. The solution penetrates the pores in TEG. The main parameters of this process are temperature and time. Raising the temperature accelerates impregnation, but the temperature should not exceed the decomposition temperature of the salt.

After impregnation, the excess solution was removed, and the impregnated TEG was dried at 80–100°C, which is well below the decomposition temperature of cobalt acetate (~200°C).

The third step was heat treatment of the impregnated TEG in air or flowing hydrogen with the aim of decomposing cobalt acetate to give cobalt oxide or cobalt metal. To assess the effects of the heat-treatment temperature and duration on the distribution and particle size of cobalt oxide or cobalt on the TEG surface, this step was carried out under different conditions:

(1) rapid heating to 500°C and holding for 1 h (cobalt oxide);

(2) thermal shock at 600°C and holding for 90 s (cobalt oxide);

(3) thermal shock at 800°C and holding for 12 s (cobalt oxide);

(4) thermal shock at 1000°C and holding for 12 s (cobalt oxide);

(5) reduction of salt-impregnated TEG powders in flowing hydrogen at 350–500°C (finely dispersed cobalt);

(6) reduction of the TEG–cobalt oxide powders in flowing hydrogen.

To characterize the composites thus prepared (phase composition; particle size and surface morphology of the support, salt, cobalt, and cobalt oxide; distribution of the particles), we used x-ray diffraction (XRD) analysis (DRON-4-07 diffractometer, filtered CoK_α radiation), scanning electron microscopy (SEM) (JEOL JSM-840 instrument equipped with a Link x-ray microanalysis system), atomic force microscopy (JEOL JEM-200CX), and Auger electron spectroscopy (AES) (LAS-2000 Riber instrument).

To follow the formation of the metallic component in TEG–metal composites and to examine the effect of each fabrication step on the microstructure and phase composition of the material, characterization was carried out after each step of sample preparation.

RESULTS AND DISCUSSION

The treatment of TEG with H_2SO_4 broadens the 002 reflection from graphite, which may be due to reintercalation or a decrease in the size of TEG crystallites. Subsequent heat treatment at 500–1000°C reduces the crystallite size. The fragmentation of graphite crystallites upon reintercalation and thermal expansion is well observed by electron microscopy and is also evidenced by the broadening of the 002 reflection from graphite (Table 1, samples 1, 2).

As seen in Fig. 1, which shows a fragment of a TEG particle after sulfuric acid oxidation and thermal shock at 800°C, the macropore (cell) size in TEG after repeat thermal expansion (1.5–2 μm) is about 3 times smaller than that in unprocessed TEG (Table 1). Moreover, the wall thickness decreases, and the surface of graphite macroplanes takes on a wavy or bumpy appearance owing to the rapid oxidizer release induced by the thermal shock.

After impregnation, water removal, and salt crystallization, we determined the phase composition and particle size (size of coherently scattering domains) of the salt.

The starting salt $Co(CH_3COO)_2$ was crystalline, as evidenced by XRD (Fig. 2). After impregnation with aqueous solutions of cobalt acetate and subsequent drying, the XRD pattern of TEG showed only the 002 reflection from graphite, pointing to a very small particle size of the salt. Moreover, in spite of the appreciable weight gain (50–70%) as a result of impregnation, no salt particles could be detected on the TEG surface by SEM (10- to 20-nm resolution). Thus, we are led to conclude that the particle size of the salt deposited on the TEG surface was below 10 nm.

The quantitative elemental composition of the samples and the thickness of the salt layer were evaluated

Table 1. Characteristics of TEG-based composite powders impregnated with cobalt acetate, heat-treated, and reduced in flowing hydrogen under different conditions

No.	Composition	Heat-treatment conditions	Phase composition	*hkl*	$\Delta 2\theta$, deg	Particle size of cobalt or cobalt oxide
1	TEG	–	TEG	002 TEG	0.4	3–5 μm (macropores)
2	TEG(H_2SO_4)	800°C, 12s	TEG	002 TEG	1.1	1–2 μm (macropores)
3	TEG + $Co(CH_3COO)_2$ (25 wt %)	800°C, 12s	TEG + Co_3O_4 (~8 wt %)			50 nm
4		Reduction in flowing hydrogen at 500°C	TEG + Co (~7 wt %)	111 Co	0.47	40 nm (min) 160 nm (mean)
5	TEG + $Co(CH_3COO)_2$ (80 wt %)	Reduction in flowing hydrogen at 500°C	TEG + Co (~30 wt %)	111 Co	0.38	50 nm (min), 500 nm
6	TEG(H_2SO_4) + $Co(CH_3COO)_2$ (80 wt %)	500°C, 12s	TEG + CoO + Co_3O_4 (~30 wt %)	–	–	–
7		800°C, 12s	TEG + CoO + Co_3O_4 (~30 wt %)	–	–	~50 nm
8		1000°C, 12s	TEG + Co_3O_4 + CoO (~30 wt %)	–	–	100 nm (min) 260 nm (mean)
9		500°C, 1 h	TEG + Co_3O_4 (~30 wt %)	–	–	100–150 nm
10		Reduction in flowing hydrogen at 500°C	TEG + Co (~25 wt %)	111 Co	0.54	60–70 nm (min) 150 nm (mean)

by AES. It was found that, in addition to carbon, oxygen, and cobalt, the material contained a minor amount of sulfur, and its surface was covered with a $Co(CH_3COO)_2$ layer whose thickness depended on the salt concentration and varied from 3 nm to tens of nanometers at salt concentrations from 25 to about 80 wt %.

The $Co(CH_3COO)_2$ layer on the TEG surface could be visualized by atomic force microscopy. Cobalt acetate was present in the form of flakes, which were barely discernible on smooth surfaces because of their small thickness. Solution accumulation in pits led to the formation of a thicker (and better structured) layer, but even in such regions its thickness did not exceed 25 nm. It seems likely that, after heat treatment, the particle size in such regions will be larger.

Thus, it follows from XRD, SEM, and AES results that, after impregnation, cobalt acetate particles are very small and are present both on the graphite surface and in pores.

As indicated above, the third step in the fabrication of TEG–metal composites is thermal decomposition of the salt. Clearly, high-temperature treatment may cause not only salt decomposition but also aggregation of metal or metal-oxide particles. For this reason, increasing the heating rate may lead to the formation of nonequilibrium, ultrafine structures.

To optimize the fabrication of TEG–metal composites, the cobalt acetate in TEG was decomposed under different conditions:

thermal shock (500, 800, and 1000°C), accompanied by the formation of cobalt oxides, and subsequent reduction of the oxides in flowing hydrogen to Co metal;

thermal decomposition of cobalt acetate at 500°C and concurrent reduction in flowing hydrogen to Co metal.

Consider the phase composition and morphology of the composites prepared with the use of thermal shocks. Upon heating, cobalt acetate decomposes according to the scheme [8]

$$Co(CH_3COO)_2 \longrightarrow CoO + (CH_3)_2CO + CO_2,$$

$$CoO + O_2 \longrightarrow Co_3O_4.$$

Heat treatment of TEG powders impregnated with cobalt acetate causes the salt to decompose to cobalt oxides. The phase composition of the product depends on the heat-treatment conditions. Thermal shock at 500°C (12 s) leads to $Co(CH_3COO)_2$ decomposition, resulting in the formation of CoO and Co_3O_4. Raising the thermal-shock temperature accelerates the thermal decomposition of the salt and the oxidation of CoO to Co_3O_4, thereby changing the phase composition of the material on the surface of the graphite support. For example, the intensity ratio of the 200 CoO and 022 Co_3O_4 XRD peaks is about 0.8 after treatment at 500

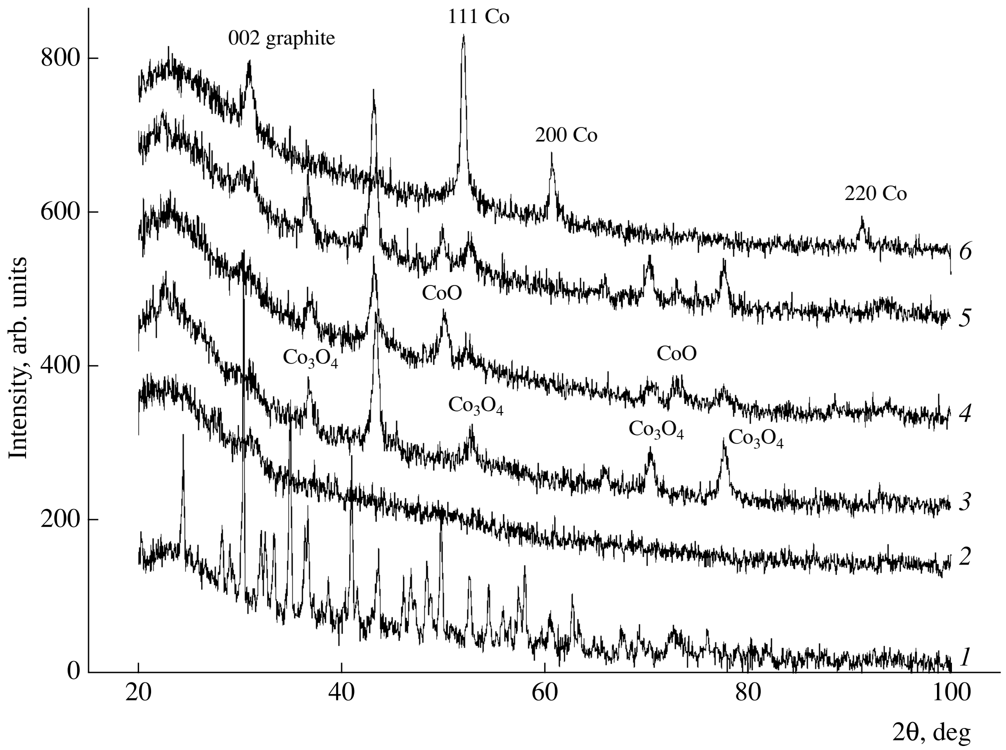

Fig. 2. XRD patterns from TEG powders oxidized with H_2SO_4, impregnated with a $Co(CH_3COO)_2$ solution, and reduced in flowing hydrogen at 500°C: (*1*) starting salt $Co(CH_3COO)_2$; (*2*) TEG impregnated with cobalt acetate and dried at 100°C (salt content ~80 wt %); (*3*–*6*) TEG + $Co(CH_3COO)_2$ heat-treated (*3*) at 500°C for 1 h, (*4*) at 800°C for 12 s, (*5*) at 1000°C for 12 s, and (*6*) at 800°C for 12 s followed by reduction to TEG + Co in flowing hydrogen at 500°C.

and 800°C and about 0.5 after treatment at 1000°C. Annealing for 1 h in air at 500°C leads to the full conversion of CoO into the spinel phase Co_3O_4 (Fig. 2). According to reference data [8], the temperature of CoO oxidation to Co_3O_4 is about 700°C. However, under the conditions of this study, Co_3O_4 forms at a lower temperature of 500°C, which is likely due to the small particle size of the CoO resulting from cobalt acetate decomposition [2].

According to AES results, thermal shocks increase the O : Co ratio in the TEG samples. This is especially pronounced in the initial stages of etching, indicating that Co_3O_4 is formed on the surface of the CoO nanoparticles. Since rapid formation of Co_3O_4 takes place at higher temperatures than $Co(CH_3COO)_2$ decomposition and coagulation of the decomposition products, the extent of CoO oxidation to Co_3O_4 is small at short annealing times.

To more accurately determine the phase composition of TEG–Co oxide materials, samples impregnated before and after heat treatment at 800°C (thermal shock and holding for 12 s, sample 3, TEG + 7 wt % Co_3O_4) were analyzed by secondary ion mass spectrometry (SIMS). The results (Table 2) demonstrate that heat treatment in air leads to the formation of cobalt oxides, oxycarbides, and hydroxides. After heat treatment in air, the Co^-, $CoOH^-$, Co_2^-, and Co_2H^- signals are stronger in comparison with the impregnated sample. These secondary ions may originate from cobalt oxides and hydroxides, which decompose under Ar^+ ion bombardment. The increase in the Co_2^+ yield attests to the formation of Co–Co bonds. The Co_2C^+, Co_2CH^+, and $Co_2CH_2^+$ peaks identified in the case of the heat-treated sample indicate that thermal shock leads to the formation of Co–C bonds through interaction between the decomposition products of $Co(CH_3COO)_2$ and the TEG surface. The presence of oxygen (heat treatment in air) results in the formation of oxycarbides. The very strong Co_2O^+, CoO^-, and CoO_2^- peaks in the spectrum of the heat-treated sample point to rapid formation of cobalt oxides. The samples subjected to a thermal shock at 800°C contained little or no sulfur, indicating that all of the sulfur (free or combined) was removed by this temperature.

Consider now the distribution of cobalt oxides over the surface of TEG particles. Rapid heating of impregnated and oxidized TEG powders to above 500°C leads to rapid oxidizer release, additional graphite expansion, and cobalt acetate decomposition into cobalt oxides. The highly nonequilibrium conditions of salt decomposition favor the formation of fine cobalt oxide particles.

Figure 3 shows SEM micrographs of TEG–$Co(CH_3COO)_2$ powders heat-treated at different temperatures.

It can be seen from Fig. 3 and Table 1 that, after oxidation of TEG with H_2SO_4 and impregnation with $Co(CH_3COO)_2$ (80 wt %), a thermal shock and subsequent holding at 800°C for 12 s lead to the formation of 50-nm cobalt oxide particles uniformly distributed over the surface of expanded TEG (poorly discernible in Fig. 3b). Increasing the shock temperature to 1000°C results in oxide particle growth: the average particle size is 260 nm (Fig. 3c), which correlates with XRD data (comparison of linewidths for cobalt oxides in samples prepared at different temperatures (Table 1). As a result of prolonged thermal annealing, fine cobalt oxide particles form aggregates about 100 nm in size (Fig. 3a) and chains even at low temperatures (500°C, 1 h, sample 9).

Thus, our results demonstrate that the optimal thermal-shock conditions for TEG powders oxidized with H_2SO_4 and impregnated with $Co(CH_3COO)_2$ are 800°C and 12 s. The short heat-treatment time eliminates the possibility of graphite oxidation and cobalt oxide aggregation. It is well known [4] that, all other factors being the same, increasing the solution concentration increases the particle size of the deposit. Comparison of TEG + $Co(CH_3COO)_2$ and TEG (oxidized with H_2SO_4) + $Co(CH_3COO)_2$ samples heat-treated at 800°C (Table 1, samples 3, 7; Fig. 3b) shows that oxidation with H_2SO_4 has little effect on the particle size, which remains at a level of 50 nm, even though the oxide content of this sample is about 4 times as high as that in sample 3. This attests to the high efficiency of the reoxidation process in reducing the particle size of oxides in TEG.

The next step—reduction of cobalt oxides to Co metal—was carried out in flowing hydrogen at 500°C for 15 h according to two schemes: during thermal decomposition of cobalt acetate or by reducing the oxides obtained by high-temperature heat treatment of impregnated TEG samples. As found by XRD analysis, all of the powder particles were covered with Co metal, independent of reduction conditions (Fig. 2).

SEM examination showed that, after reduction during thermal decomposition, cobalt was present in the form of spherical particles uniformly distributed over the surface of the TEG particles and in macropores. It was found that decreasing the metal concentration reduced the particle size, in agreement with earlier results [2–4]. At a cobalt content of 7 wt % (sample 4), the minimum particle size was about 40 nm (Fig. 4a), and the mean particle size was 160 nm. Large particles, up to 400 nm in size, were sometimes also encountered but were very rare. The separation between the particles was 80 nm, and they were distributed over the surface rather uniformly, although there were areas 400 × 400 nm containing no cobalt. In some areas, Co particles were arranged in the form of straight chains (most likely, owing to the attachment of Co particles to the edges of graphite macroplanes) 5–7 μm in length. In the case of the TEG–Co (30 wt % Co) composite (sample 5), we observed larger cobalt particles: spherical particles about 500 nm in size and a very small amount of 50-nm particles (Fig. 4b).

Table 2. Yield of singly charged ions (SIMS, calibration against carbon)

Mass	Element/compound	Yield of singly charged ions	
		TEG + $Co(CH_3COO)_2$ (25 wt %)	TEG + Co_3O_4 (7 wt %)
		Positive ions	
1	H	1020	3421
2	H_2	33	123
16	O	23	272
59	Co	2950	48048
71	CoC	103	227
75	CoO	11	342
76	CoOH	9	165
83	CoC_2	21	60
87	CoCO	27	24
88	CoCOH	7	24
91	CoO_2	39	21
95	CoC_3	13	8
99	CoC_2O	1	44
103	$CoCO_2$	13	97
115	CoC_2O_2	887	1172
118	Co_2	55	4335
119	Co_2H	1	39
130	Co_2C	7	81
134	Co_2O	3	353
142	Co_2C_2	0	21
		Negative ions	
1	H	2890	12444
2	H_2	0	6
16	O	2920	22279
75	CoO	5	263
76	CoOH	3	112
91	CoO_2	3	801
92	CoO_2H	0	48

Similar results were obtained by reducing TEG samples that were heat-treated after oxidation and impregnation. At the same time, at a Co content of 30 wt % (sample 10), the mean particle size was notably smaller, 150 nm (Fig. 4c). The 111 Co peak from

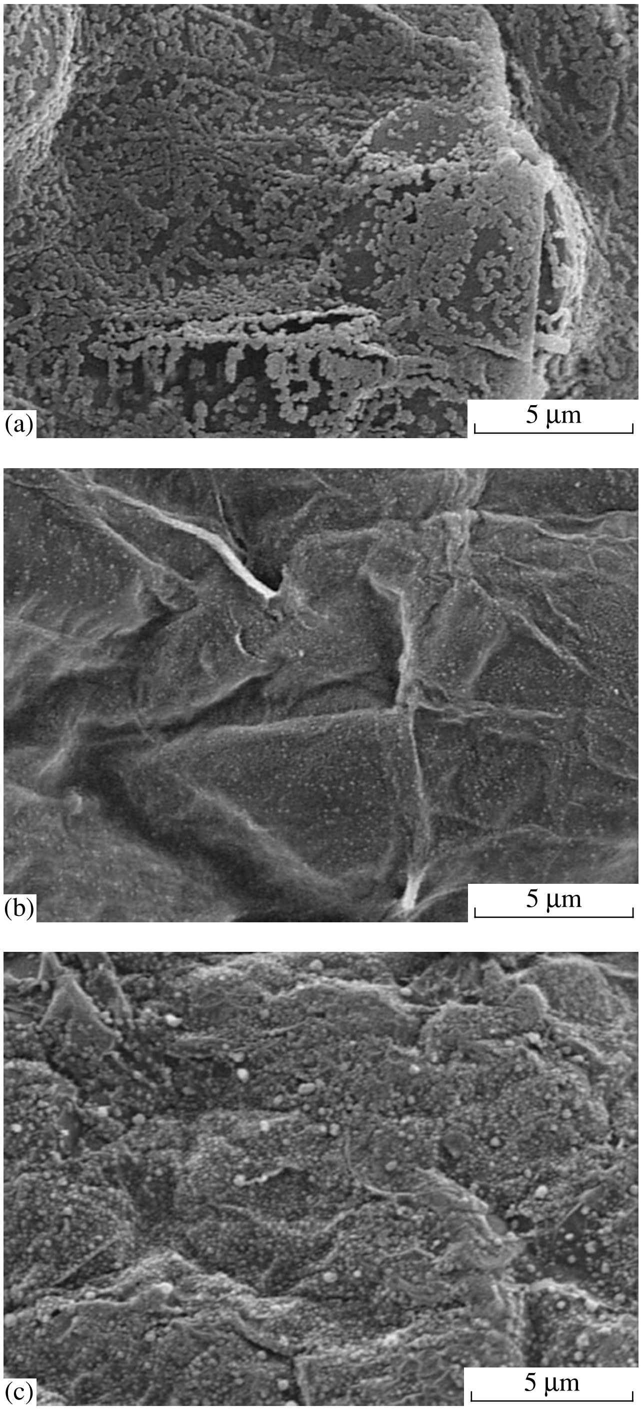

Fig. 3. TEG particles after oxidation with H_2SO_4, impregnation with $Co(CH_3COO)_2$, and heat treatment under different conditions: (a) 500°C, 1 h; (b) 800°C, 12 s; (c) 1000°C, 12 s.

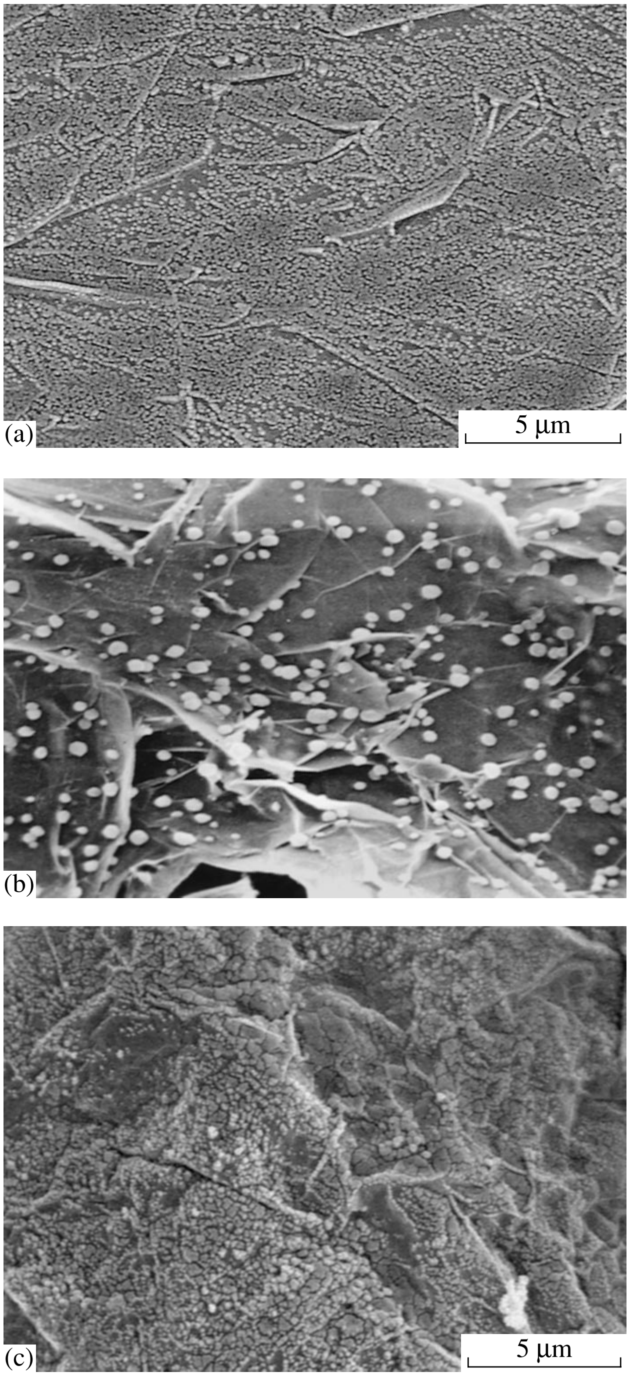

Fig. 4. TEG particles after impregnation with $Co(CH_3COO)_2$ and reduction in flowing hydrogen at 500°C: (a) direct reduction, ≃7 wt % Co (sample 4); (b) direct reduction, ≃30 wt % Co (sample 5); (c) reduction after oxidation with H_2SO_4, impregnation with $Co(CH_3COO)_2$, and thermal shock at 800°C (≃30 wt % Co, sample 10).

sample 10 was about twice as broad as that from sample 5, which was reduced during salt thermolysis.

Figure 5 shows the size distributions of cobalt particles in TEG–Co composites prepared by different procedures. It can be seen that, at low Co concentrations (7 wt %), and also after TEG oxidation with sulfuric acid, impregnation with a cobalt acetate solution, a thermal shock at 800°C, and reduction in flowing hydrogen, most of the particles are from 140 to 160 nm in size. In the composites prepared via TEG impregna-

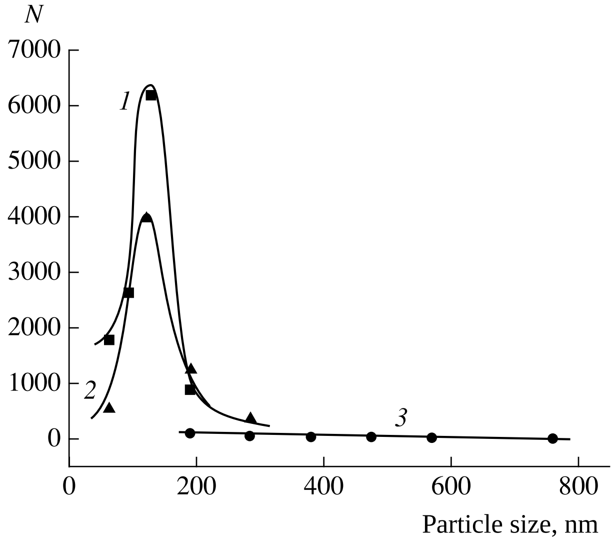

Fig. 5. Size distributions of cobalt particles (300-μm^2 area): (*1*) direct reduction, ≃7 wt % Co (sample 4); (*2*) reduction after oxidation with H_2SO_4, impregnation with $Co(CH_3COO)_2$, and thermal shock at 800°C (≃30 wt % Co, sample 10); (*3*) direct reduction, ≃30 wt % Co (sample 5) (see micrographs in Figs. 4a–4c).

tion with a cobalt acetate solution and subsequent thermolysis in flowing hydrogen, the particles range in size from 200 to 800 nm.

CONCLUSIONS

The formation of nanostructured TEG–Co composites was studied by XRD and electron microscopy. The results demonstrate that the pretreatment of TEG in H_2SO_4 leads to the formation of oxygen-containing surface groups, which act as exchange centers for fixing cations on the graphite surface during impregnation with a cobalt acetate solution. In addition, heat treatment of oxidized graphite gives rise to additional expansion and reduces its particle size.

TEG impregnation with cobalt acetate and subsequent drying result in the formation of a fine-grained salt film from 3 nm to tens of nanometers in thickness at salt concentrations from 25 to about 80 wt %.

Decomposition of the salt as a result of a thermal shock leads to the formation of fine cobalt oxide particles on the TEG surface. The particle size varies from 50 to 100–250 nm, depending on the heat-treatment temperature and duration, impregnation conditions, and Co content: higher heat-treatment temperatures and salt concentrations result in a larger size of oxide particles. Pretreatment in sulfuric acid reduces the crystallite size of the graphite matrix and, all other factors being the same, the size of the metal or metal-oxide particles.

Subsequent reduction of the cobalt oxides in flowing hydrogen yields cobalt particles. Their size and distribution over the support surface depend on Co concentration. At low Co contents (≤10 wt %), the particle size is 40–150 nm. At higher Co contents (up to 30 wt %), the minimum particle size is 60–70 nm, and the mean particle size is 150 nm; large, aggregated particles, up to 400 nm in size, are also present in significant amounts.

ACKNOWLEDGMENTS

This work was supported by the Science and Technology Center of Ukraine, project no. 1618.

REFERENCES

1. Bukhtiyarov, V.I. and Slin’ko, M.G., Metallic Nanosystems in Catalysis, *Usp. Khim.*, 2001, vol. 70, no. 2, p. 167.
2. Shpak, A.P., Kunitskii, Yu.A., and Karbovskii, V.L., *Klasternye i nanostrukturnye materialy* (Nanostructured and Clustered Materials), Kiev: Akademperiodika, 2001.
3. Sergeev, G.B., Nanochemistry of Metals, *Usp. Khim.*, 2001, vol. 70, no. 10, p. 915.
4. *Catalyst Supports and Supported Catalysts: Theoretical and Applied Concepts*, Stiles, A.B., Ed., Boston: Butterworths, 1988. Translated under the title *Nositeli i nanesennye katalizatory. Teoriya i praktika*, Moscow: Khimiya, 1991.
5. King Lun Yeung and Eduardo, E.W., A Scanning Tunneling Microscopy Study of the Platinum Catalyst Particles Supported on Graphite, *J. Vac. Sci. Technol., B*, 1991, vol. 9, no. 2, pp. 798–803.
6. Dong Jin Sun, Tae Jin Park, and Son-Ki Ihm, Effect of Surface Oxygen Groups of Carbon Supports on the Characteristics of Pd/C Catalysts, *Carbon*, 1993, vol. 31, no. 3, pp. 427–435.
7. Khar’kov, E.I., Lysov, V.I., Matzui, L.Yu., *et al.*, Ukr. Patent 33777A. *Byull. Izobret.*, 2001, no. 1.
8. Antonova, M.M. and Brakhnova, I.T., *Svoistva elementov* (Properties of Elements), Moscow: Metallurgiya, 1976, part 2.